

Accelerating Unsteady Fluid Dynamic Simulations for Microdevices for Droplet Generation Using Singular Value Decomposition and Recurrent Neural Network

Atsuto Nishihata, Osamu Tonomura*, Ken-ichiro Sotowa

Dept. of Chem. Eng., Kyoto University, Nishikyo, Kyoto 615-8510, Japan
tonomura@cheme.kyoto-u.ac.jp

Digital twins are expected to be applied in the chemical process industry as important technology for improving productivity and profits. A key requirement is a flow model that reproduces the internal flow of equipment. Computational fluid dynamics (CFD) provides high-fidelity field data and is widely used to analyze flow and mass transfer, but unsteady simulations are computationally expensive because the solution must be advanced with very small time steps. To integrate CFD into digital twins, this cost must be reduced. In this study, the reduced order modelling (ROM) of CFD using singular value decomposition and recurrent neural network was applied to a T-shaped microdevice for droplet generation, which is used in particle production and related applications. The resulting ROM accurately predicts flow fields and droplet size across operating conditions while achieving an approximately 3,600-fold speed-up relative to CFD. Novelty is the implementation of a CFD-trained ROM as a digital-twin virtual sensor for microdroplet devices. The method enables near-real-time droplet-size estimation with demonstrated accuracy and robustness.

1. Introduction

Particles with uniform size and shape are used as functional materials in biopharmaceuticals, electrical and optical devices, catalysts, etc. In recent years, the use of microdroplets for particle synthesis has attracted attention because it is possible to produce particles with a narrow particle size distribution (Wang et al., 2017, Batyrgazieva et al., 2018). In microdroplet technology, two immiscible liquids are fed into microchannels of micrometers or millimeters, and the dispersed phase fluid is generated as droplets in the continuous phase fluid. At this time, a uniform shear force from the continuous phase acts on the dispersed phase, resulting in the generation of droplets of uniform size and shape. The main microdevices for generating microdroplets are T-junction type, co-flow type, and flow-focusing type (Li et al., 2018). Droplet size is an important factor that determines particle functions, since it affects the flow and diffusion of materials within the droplet and the reaction rate (Liu et al., 2021). Therefore, there is a demand for droplet size measurement and control technology. Previous studies have reported methods for measuring droplet size based on the change in diffraction intensity (Nguyen et al., 2006) when light is shone onto a droplet, and on images taken with a high-speed camera (Srikanth et al., 2021). Furthermore, black-box models that represent the relationship between operating conditions and droplet size (e.g., Mahdi and Daoud, 2017) have the potential to be applied to virtual measurements, even though they were developed for equipment design. However, because these are data-driven models, they are highly dependent on the equipment and can become unstable when extrapolating near the transition point of the droplet generation mechanism. In recent years, detailed physical models, such as computational fluid dynamics (CFD), have become available. CFD analysis of the droplet generation process has the greatest strength in its ability to represent interfacial phenomena and quantify various state variables that are difficult to measure, and its usefulness has been reported (e.g., Soh et al., 2016). Although different from microdevices, virtual measurements using CFD have been developed for measuring the temperature and heat flux of combustion furnaces (Aversano et al., 2021) and the thermal flow field of fluidized beds (Li et al., 2024). However, to the best of our knowledge, explicitly framing CFD for T-junction microdevices as virtual sensors for droplet size measurement has not been reported.

Computer-aided engineering (CAE) simulation, which utilizes numerical analysis such as CFD, has long been introduced in the fields of product design and research and development (R&D). In recent years, new technologies such as the Internet of Things (IoT) and artificial intelligence (AI) are being introduced to product design and manufacturing sites. Against this background, attempts are being made to integrate conventional CAE technology with AI and IoT technology. In order to advance such attempts, this study aims to develop a virtual sensor for measuring the flow conditions in the microdevice for chemical processes, and the final goal is to apply the developed virtual sensor to a digital twin system. If the digital twin of the chemical process is realized, it will be possible to numerically visualize what is happening in the operating equipment, monitor the internal state of the equipment that cannot be detected with sensors, predict the occurrence of abnormalities, and enable timely control and adjustment to optimal conditions, which is expected to lead to cost reductions and quality improvements. However, CFD, especially for unsteady flows such as droplet generation processes, is computationally expensive because it must march the flow solution with a small step in time. Introducing CFD into digital twins, there is a need to reduce the above cost and make unsteady CFD more affordable.

In this study, a digital twin is interpreted as a cyber-physical framework that synchronizes equipment data with physics-based models to enable monitoring, prediction, and control. Within this framework, a virtual sensor estimates quantities that are difficult to measure directly (e.g., droplet size) from readily available inputs (e.g., flow rates) fast enough for decision-making. To realize this virtual sensor, a CFD-trained reduced-order model (ROM) is constructed for a T-shaped microdevice for droplet generation: CFD fields are dimensionally compressed via singular value decomposition (SVD) and temporal dynamics are learned using a recurrent neural network (RNN). Prediction accuracy and inference time are quantified, ROM outputs are compared against full CFD to demonstrate rapid virtual measurement of droplet size, and implications for deploying CFD within digital twins are discussed.

2. T-shaped channel for droplet generation: CFD simulation settings and results

A T-shaped channel shown in Fig. 1a is taken up in this study. The channel material is polydimethylsiloxane (PDMS), and silicone oil (293 K) is supplied from the inlet as the continuous phase and water (293 K) as the dispersed phase. The silicone oil and water are mixed at the T-junction and are sent to the outlet, but the water disperses as droplets in the silicone oil within the hydrophobic channel. Fig. 1b shows the overall diagram of the experimental setup. Silicone oil (Momentive, 10cSt) and water (Merck, Direct-Q UV 3) were pumped into the device (Fukoku Bussan) with the T-shaped channel shown in Fig. 1a using syringe pumps (Harvard, PHD ULTRA). The syringe pumps and device were connected using silicone tubes (inner diameter: 0.5 mm, outer diameter: 1 mm). The T-junction was observed from above with a digital microscope (Keyence, VH-Z75).

In this study, three-dimensional CFD simulations were employed to analyze the fluid flow in the T-shaped microdevice for droplet generation. Mathematical model of the microdevice and simulation settings are as follows: the equations used to describe the system are the Navier-Stokes (Eq. (1)) and continuity equations (Eq. (2)). The liquid-liquid interface is resolved using the volume-of-fluid (VOF) model (Eq. (3)). In Eq. (3), F represents the volume fraction of a substance in the cell. The VOF method is a method for expressing the free interface in multiphase flow, and the density ρ in the cell is expressed by Eq. (4) using the densities of silicone oil and water, which are given by ρ_o and ρ_w , respectively.

$$\frac{\partial v}{\partial t} + (v \cdot \nabla)v = -\nabla p + \frac{1}{Re} \nabla^2 v \quad (1)$$

$$\frac{\partial \rho}{\partial t} + \nabla \cdot (\rho v) = 0 \quad (2)$$

$$\frac{\partial F}{\partial t} + v \cdot \nabla F = 0 \quad (3)$$

$$\rho = F\rho_o + (1 - F)\rho_w \quad (4)$$

In all cases studied, the flow was simulated by laminar model, while adiabatic conditions were applied at domain boundaries. Slip effects were negligible. The two liquid phases in the microdevice were assumed to have the physical properties of water (293K) and silicone oil (293K). Unless otherwise stated all simulations were performed in three dimensions. Simulations were performed using ANSYS Fluent. The inlet linear velocity of water was fixed at $v_w = 0.085$ m/s, and the inlet linear velocity of silicone oil v_o [m/s] was varied. The cells for discretizing the space were cubes with sides of 2 μm . The semi-implicit method for pressure linked equations-consistent (SIMPLEC) was implemented for pressure-velocity coupling and the spatial discretization was performed using the second order upwind scheme. An unsteady simulation was performed under a time step of 1.0×10^{-5} s until 0.01 seconds has elapsed, which is equal to the mean residence time of the fluid.

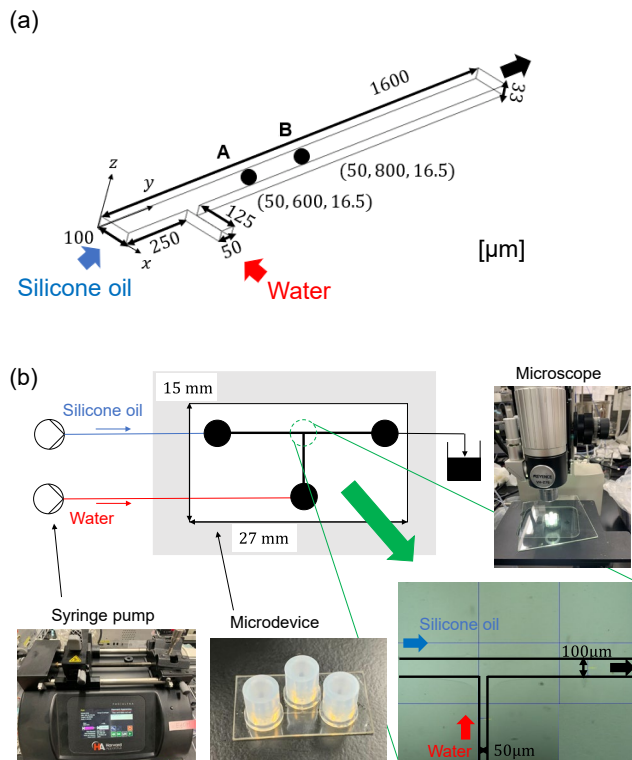


Figure 1: T-shaped channel (a) schematic diagram and (b) experimental setup.

Fig. 2a shows the droplet generation process when the water-to-oil flow rate ratio $Q_w/Q_o = 0.28$, and water is subjected to shear force by silicone oil, and droplets are generated because of low wettability with respect to the wall. To measure the droplet size, the arrival times of each droplet at two points A and B in the channel shown in Fig. 1a were measured. Fig. 2b shows the droplet size (L), which is non-dimensionalized by channel width (W), obtained by CFD, the experiment of the previous study (Garstecki et al., 2006), and the experiment conducted in this study against Q_w/Q_o [-]. The results showed that the droplet size increased with an increase in Q_w/Q_o . This is because when the flow rate of the dispersed phase is fixed, the shear force on the dispersed phase decreases as the flow rate of the continuous phase decreases. Since the CFD results are close to the experimental results, it is shown that CFD simulation is useful for the T-shaped device for droplet generation. However, the unsteady calculation based on CFD requires about 6 hours of calculation time for one operating condition. To utilize CFD for virtual measurement of droplet generation, it is necessary to shorten the calculation time to a few seconds, and the construction of an ROM is investigated in the next section.

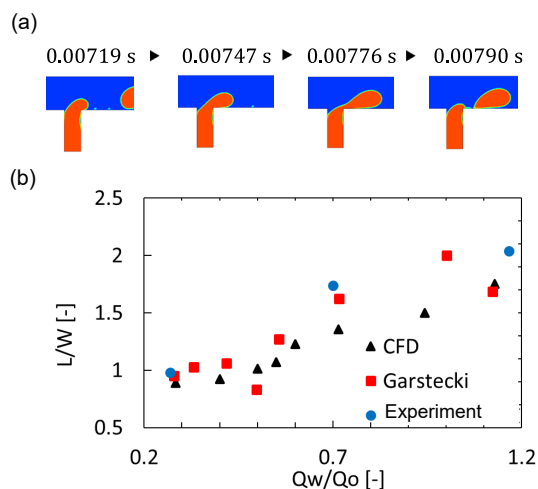


Figure 2: Droplet size (a) droplet generation process by CFD and (b) validation of CFD against experiment and published trends

3. Reduced order modeling and its results

3.1 SVD and RNN

In this study, the ROM was constructed using SVD and RNN. As for SVD, dimensionality reduction was performed on the n dimensional, n_t step time series data $\mathbf{X} = [x_1, x_2, \dots, x_{n_t}]$ ($\mathbf{X} \in \mathbb{R}^{n \times n_t}$) that represents the flow field. The eigenvalues of the covariance matrix $\mathbf{X}\mathbf{X}^T \in \mathbb{R}^{n \times n}$ were calculated, but in this study, $n \approx O(10^6)$, which is computationally expensive. Therefore, the eigenvalues were calculated by solving the eigenvalue problem of $\mathbf{X}^T\mathbf{X} \in \mathbb{R}^{n_t \times n_t}$, which is the transposed matrix of $\mathbf{X}\mathbf{X}^T$. The SVD in Eq. (5) decomposes the time series data into \mathbf{U} and $\mathbf{\Sigma}$, which are time-independent, and \mathbf{V}^T which is time-dependent.

$$\mathbf{X} = \mathbf{U}\mathbf{\Sigma}\mathbf{V}^T \quad (5)$$

Here, r is the rank of \mathbf{X} , $\mathbf{U} \in \mathbb{R}^{n \times r}$ and $\mathbf{V} \in \mathbb{R}^{r \times n_t}$ are orthogonal matrices, and $\mathbf{\Sigma} \in \mathbb{R}^{r \times r}$ is a diagonal matrix with singular values on the diagonal elements (Calka et al., 2021). Dimensionality reduction was performed by selecting singular values in order from the largest basis number to the specified basis number. Furthermore, RNN was used to model the relationship in which changing the operating conditions shifts the flow field inside the device, which in turn changes the droplet size. CFD simulations were performed for scenarios that changed the operating conditions, and the results of SVD on the obtained flow fields were used as training data for the RNN to learn the time-dependent terms of the RNN. The activation function used was the sigmoid function, and the gradient descent method was used for optimization (Calka et al., 2021). In this study, ANSYS Dynamic ROM Builder, which is accessible in the ANSYS Twin Builder, was used to perform the calculations mentioned above.

3.2 Results and discussion of ROM for microdevice

ROM was constructed using the CFD simulation results for five conditions of $Q_w/Q_o = 0.35, 0.39, 0.45, 0.50,$ and 0.55 as training data, and the droplet size was measured. As shown in Fig. 3, when the basis number was 20, the density distribution by the ROM and the density distribution by CFD were significantly different, so the data description capacity was low. Therefore, the basis number was increased to 50 and the ROM was reconstructed, and named ROM1. Fig. 4 shows a comparison of the measurement results by CFD simulation under the flow rate conditions used for training, the measurement results by CFD simulation under the conditions used for verification, and the measurement results by ROM1-based simulation. It was shown that the droplet size measurement results were close between CFD and ROM1. The mean square error between CFD and ROM1 was 5.02×10^{-3} [-]. In addition, a three-dimensional unsteady simulation for 0.01 seconds required to measure droplet size under one flow rate condition required about 6 hours of calculation time in the case of CFD. On the other hand, it took about 6 seconds to calculate using ROM. In other words, the calculation time was reduced to 1/3600 by constructing ROM.

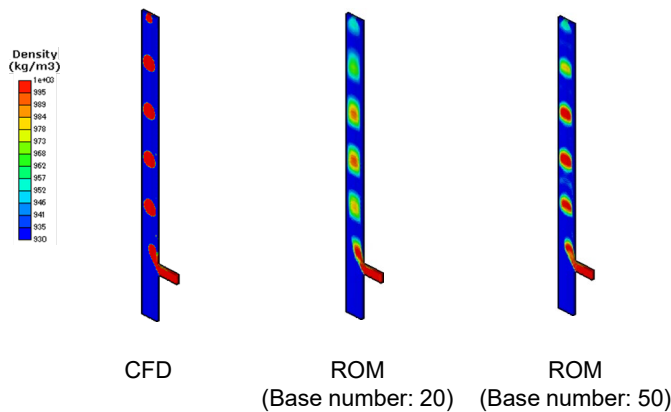


Figure 3: A schematic diagram of T-shaped channel

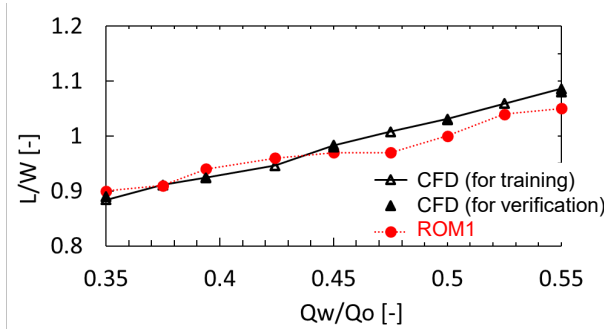


Figure 4: Comparison of droplet size measurements using CFD and ROM1 — validation at trained and unseen conditions

An ROM was constructed by removing the condition $Q_w/Q_o = 0.39$ from ROM1, and named it ROM2. Fig. 5 shows a comparison of the measurement results by CFD simulation under the flow rate conditions used for training, the measurement results by CFD simulation under the conditions used for verification, and the measurement results by ROM2-based simulation. The mean square error between CFD and ROM2 was 1.04×10^{-2} [-]. In the case of ROM2, the number of CFD simulation results for training was reduced, resulting in a large error around $Q_w/Q_o = 0.40$, which predicted a larger droplet size than the CFD. This suggests that in order to build a high-precision ROM that faithfully reproduces the process, it is important to not only increase the number of bases, but also to select CFD simulation conditions according to the process characteristics.

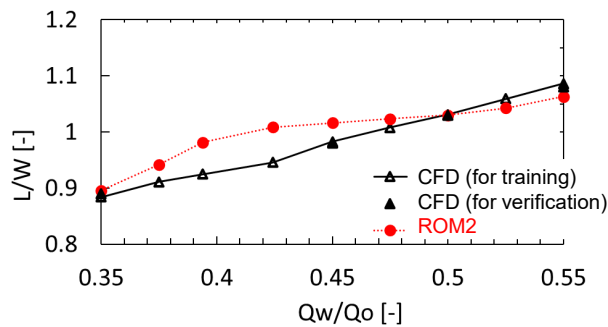


Figure 5: Comparison of droplet size measurements using CFD and ROM2 — validation at trained and unseen conditions

The results mean the ROM1 can be used in a digital twin: it is accurate, runs quickly enough to support decisions, and still performs well on new operating conditions. The ROM2 test also shows what training coverage is needed around regime changes.

4. Conclusions

A reduced order model (ROM) for a T-shaped microdevice for droplet generation was constructed by compressing CFD fields via singular value decomposition (SVD) and learning temporal dynamics with a recurrent neural network (RNN). The ROM reproduced device flow conditions approximately 3,600 times as fast as CFD and predicted droplet size with comparable accuracy, enabling near-real-time virtual measurement. The framework is directly extensible to reaction/separation microdevices and to deployment within a digital twin loop with periodic online calibration and supervisory control.

Nomenclature

L – droplet size, m
 n – dimension, -
 n_t – time step, -
 o – silicone oil, -
 p – pressure, Pa
 Q – flow rate, m^3/s
 r – dimension, -

Re – Reynolds number, -
 t – time, s
 v – velocity, m/s
 W – channel width, m
 w – water, -
 ρ – liquid density, kg/m^3

Acknowledgments

This work was partially supported by the Grant-in-Aid for Scientific Research (B) (No. 23H01754) and a project, Development of Continuous Production and Process Technologies of Fine Chemicals, commissioned by the New Energy and Industrial Technology Development Organization (NEDO).

References

- Aversano, G., Ferrarotti, M., Parente, A. 2021, Digital twin of a combustion furnace operating in flameless conditions: reduced-order model development from CFD simulations. *Proceedings of the Combustion Institute*, 38(4), 5373-5381.
- Batyrkazieva, D.R., Khudeev, I.I., Guseva, E.V., Menshutina, N.V., Dorokhov, I.N. 2018, The Study of Microbiological processes on microfluidic chips and modeling. *Chemical Engineering Transactions*, 70, 1771-1776.
- Calka, M., Perrier, P., Ohayon, J., Grivot-Boichon, C., Rochette, M., Payan, Y. 2021, Machine-learning based model order reduction of a biomechanical model of the human tongue. *Computer Methods and Programs in Biomedicine*, 198, 105786.
- Garstecki, P., Fuerstman, M.J., Stone, H.A., Whitesides, G.M. 2006, Formation of droplets and bubbles in a microfluidic T-junction—scaling and mechanism of break-up. *Lab on a Chip*, 6(3), 437-446.
- Li, W., Zhang, L., Ge, X., Xu, B., Zhang, W., Qu, L., Choi, C.H., Xu, J., Zhang, a., Lee, H., Weitz, D.A. 2018, Microfluidic fabrication of microparticles for biomedical applications. *Chemical Society Reviews*, 47(15), 5646-5683.
- Li, X., Xu, Q., Wang, S., Luo, K., Fan, J. 2024, A novel data-driven reduced-order model for the fast prediction of gas-solid heat transfer in fluidized beds. *Applied Thermal Engineering*, 253, 123670.
- Liu, Y., Zhao, Q., Yue, J., Yao, C., Chen, G. 2021, Effect of mixing on mass transfer characterization in continuous slugs and dispersed droplets in biphasic slug flow microreactors. *Chemical Engineering Journal*, 406, 126885.
- Mahdi, Y. and Daoud, K. 2017, Microdroplet size prediction in microfluidic systems via artificial neural network modeling for water-in-oil emulsion formulation. *Journal of Dispersion Science and Technology*, 38(10), 1501-1508.
- Nguyen, N.T., Lassemono, S., Chollet, F.A. 2006, Optical detection for droplet size control in microfluidic droplet-based analysis systems. *Sensors and actuators B: Chemical*, 117(2), 431-436.
- Soh, G. Y., Yeoh, G.H., Timchenko, V. 2016, Numerical investigation on the velocity fields during droplet formation in a microfluidic T-junction. *Chemical Engineering Science*, 139, 99-108.
- Srikanth, S., Raut, S., Dubey, S.K., Ishii, I., Javed, A., Goel, S. 2021, Experimental studies on droplet characteristics in a microfluidic flow focusing droplet generator: effect of continuous phase on droplet encapsulation. *The European Physical Journal E*, 44(8), 108.
- Wang, J., Li, Y., Wang, X., Wang, J., Tian, H., Zhao, P., Tian, Y., Gu, Y., Wang, L., Wang, C. 2017, Droplet microfluidics for the production of microparticles and nanoparticles. *Micromachines*, 8(1), 1-22.